Effects of Fuel Content and Density on the Smoldering Characteristics of Cellulose and Hemicellulose

Benjamin D. Smucker[a], Tejas C. Mulky[a], Daniel A. Cowan[a], Kyle E. Niemeyer[a], David L. Blunck[a,*]

[a]*School of Mechanical, Industrial, and Manufacturing Engineering, Oregon State University, Corvallis, Oregon, USA*

Abstract

Smoldering combustion in wildland fires poses hazards for both ecosystems and humans by destroying biomass, transitioning to flaming combustion, and releasing significant quantities of pollution. Understanding the parameters that control smoldering is necessary to help predict and potentially mitigate these hazards. A challenge in identifying these parameters is the wide variety of biomasses which occur in nature. The objective of this study is to identify the effects of density and fuel concentration on the smoldering characteristics of cellulose and hemicellulose mixtures. These fuels were considered because they are some of the major organic constituents within biomass. To this end, downward smoldering propagation velocities were measured for 50%, 75%, and 100% cellulose content at densities varying from 170 to 400 kg/m^3). The horizontal smoldering propagation velocities and temperature distributions were also determined for loosely packed samples ranging from 100% to 0% cellulose (with residual hemicellulose). Additionally, horizontal smoldering propagation velocities were determined for systematically varied ratios of cellulose (50% to 100%) and densities (200 to 400 kg/m^3). The fuel was burned in an insulated reactor box. An infrared camera measured the horizontal propagation velocity, and thermocouples measured the downward propagation. A one-dimensional reactive porous media model with reduced chemistry was used to identify key processes causing the observed sensitivities. At constant packing density, the propagation velocity increased as cellulose content decreased because of decreased heat release with increased cellulose content and the earlier onset of hemicellulose pyrolysis. The propagation velocity decreased with respect to packing density when the fuel content was constant because of reduced oxygen diffusion. The propagation velocity increased with cellulose content when the fuel was loosely packed because of the decreasing density.

Keywords: Wildland Fires, Smoldering, Solid Combustion

*Corresponding author

Email address: david.blunck@oregonstate.edu (David L. Blunck)

1. Introduction

Smoldering wildland fires pose several hazards that differ from those of flaming combustion [1]. In comparison, smoldering can release larger quantities of smoke, carbon monoxide, and volatile organic compounds (VOCs). The greater release of pollutants stems from the lower temperatures and incomplete combustion associated with smoldering [2–6]. Smoldering can persist for much longer periods of time than flaming combustion, and can transition to flaming which then spread more rapidly [1]. The detrimental effects of smoldering combustion have motivated research into the sensitivity of this mode of combustion to parameters such as density, moisture content, inorganic content, and composition of the fuel.

Combustion limits and propagation velocities of smoldering depend on moisture content, inorganic content, and packing density [7–10]. For example, increased moisture and increased packing density (ρ) in peat both decrease the propagation velocity (v_h) of the smoldering front. Similarly, in cotton increased packing density decreases the smoldering propagation [11, 12]. However, sensitivity to density is dependent on moisture content [10], indicating a coupling between the parameters that affect the propagation velocity.

Smoldering characteristics can change significantly depending on the origin of the biomass [7, 13, 14]. This can challenge the forecasting of smoldering characteristics if the specific fuel and conditions have not been evaluated. For example, samples of biomass collected from across North America had limiting moisture contents (for sustained smoldering) that varied from 40% to higher than 100%, depending on the composition of the plant litter [7]. Further illustrating the sensitivity to the fuel, smoldering of cotton (ρ =100 kg/m^3) propagates at about 1.5 mm/min, but dry peat at a similar density propagates at velocities near 0.7 mm/min [10, 11].

A notable difference between fuels is the chemical composition and the associated reaction characteristics. The three primary organic compounds in plant litter are cellulose, hemicellulose, and lignin. The ratio of each component in the litter changes with the source of the fuel and amount of decomposition [15]. Cellulose, hemicellulose, and lignin have different pyrolysis and oxidation characteristics [8], so it is expected that they influence the smoldering characteristics of biomass differently. Thermogravimetric analysis has shown that lignin pyrolyzes slowest and reacts over the largest temperature range of the three constituents [16, 17]. Hemicellulose and cellulose pyrolyze at similar rates, but hemicellulose has a lower activation energy and begins to pyrolize at a lower temperature [18, 19].

Further knowledge about the smoldering characteristics (i.e., propagation velocities) of cellulose, hemicellulose, and lignin is needed to help develop a more universal understanding of smoldering characteristics for a broad range of biomass. With this background and motivation, the objective of this study is to identify the effects of density and fuel concentration on the smoldering characteristics of mixtures of cellulose and hemicellulose using both experimental and computational methods. Future work will consider the influence of lignin, but it is outside of the scope of this work. It is expected that the key chemical and physical processes identified can ultimately provide insights into the smoldering characteristics of biomass, depending on the density and the concentrations of cellulose and hemicellulose.

2. Experimental Approach

The experimental arrangement (shown in Fig. 1) consisted of an instrumented reactor box and an infrared (IR) camera. The reactor box was 20 cm × 20 cm × 10 cm and contained the powderized fuel (cellulose/hemicellulose mixtures). The walls of the reactor box were made of calcium silicate insulation board. The infrared (IR) camera (FLIR SC6700) acquired images reflected off of a polished stainless steel mirror placed 75 cm above the reactor box. Polished stainless steel has an emissivity of roughly 0.1 and is much cooler than the fuel sample. Consequently, emission from the mirror is minimal. The IR camera was mounted approximately 100 cm horizontally from the mirror.

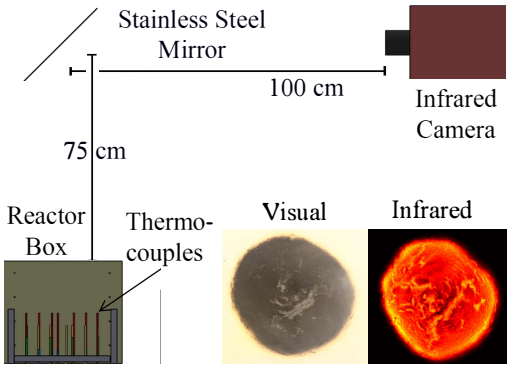

Figure 1: Experimental arrangement for measuring the smoldering propagation velocities during smoldering combustion. The images in the bottom right corner are visual and infrared images of the same burn (75% cellulose, ρ = 250 kg/m^3) approximately 50 minutes after ignition. The burned area is approximately 10 cm across.

An additional reactor was used to study downward smoldering propagation for some of the tests. This

allowed evaluation of a one-dimensional smoldering model and experimental comparison of downward and horizontal smoldering. The reactor was 10 cm × 10 cm × 13 cm deep. The thermocouples were placed in the center of the reactor, and spaced 1 cm apart starting 1 cm below the surface of the fuel.

The fuel content and density were systematically changed to allow sensitivity of smoldering propagation to fuel content and density to be identified. Initially, the fuel content was varied from 100% to 0% cellulose (with the remainder being hemicellulose). Cellulose and hemicellulose were selected because they are primary constituents of biomass. The smoldering characteristics of lignin will be considered in future studies.

The density of the fuel inherently varied between different mixtures because cellulose and hemicellulose had different loose packing densities. The density of the pure hemicellulose (loosely packed ~720 kg/m^3) was about four times greater than the density of the pure cellulose (loosely packed ~170 kg/m^3). To isolate chemistry effects and minimize density effects, the density was held constant while the fuel content was varied from 50% to 100% cellulose by mass for some tests. This range was selected to achieve constant densities. When the cellulose content was less than about 40%, it was not physically possible to achieve densities consistent with the 100% cellulose case. To identify density effects, the density was varied while the fuel content was held constant. Fuels with 50%, 75%, and 100% cellulose content were tested with densities ranging from 200–400 kg/m^3. While these densities are outside of the range of natural fuels, such as peat and cotton [8, 12], they are beneficial for helping to identify the influence of density on smoldering behavior for the target fuels.

The cellulose evaluated was α-cellulose (obtained from Sigma-Aldrich), sized such that less than 20% was retained by 35 U.S. Standard Mesh (500 µm), greater than 50% passed 100 Mesh (150 µm), and greater than 35% passed 200 Mesh (75 µm). The hemicellulose was powderized glucomannan extracted from konjac root (obtained from Nutricost). The glucomannan particles ranged from 125 to 75 µm. The fuel was mixed using a tumbler for at least 5 minutes and packed in the reactor box to the desired density.

The fuel was ignited in the center of the reactor using a 20 W cartridge heater (diameter = 0.64 cm for both the horizontal and vertical reactors.) The temperature of the heater was controlled using a temperature controller. The heater was placed into the fuel once it reached approximately 400 °C and allowed to heat to 550 °C. These conditions ignited the fuel the most consistently. The cartridge heater was removed once the propagation front was self-sustaining. The burns typically lasted 1–5 h. Any fuel that adhered to the heater was scraped back into the center of the box.

The thermocouples took temperature readings with a frequency of 1 Hz. The ignition temperature (rather than peak temperature) was used to determine the propagation velocity to avoid bias from changes in peak temperature with depth. The vertical propagation velocities reported are the average values determined from 3–6 cm below the surface of the fuel. An exception is the propagation velocity for 100% cellulose at 300 kg/m^3. It is averaged from 3 to 4 cm below the surface, as the smoldering front extinguished below 4 cm.

Data was collected using the IR camera at a frequency of 0.1 Hz. The IR camera (FLIR SC6700) had an integration time equal to 4.8×10^{-4} ms for each image. The IR camera was sensitive to wavelengths from 1 to 5 µm. The spatial resolution was typically 0.335 mm/pixel.

Horizontal smoldering propagation velocities were determined from the infrared images. The fuel was considered to be smoldering at a pixel if the photon count surpassed 1800. This value was selected because it was determined experimentally that this photon count corresponds to the temperature necessary for the smoldering front to self-propagate. Once a pixel "ignited" it was considered ignited for the duration of the burn to account for regions that cooled after burning. The area of the burn was determined for each image based on the number of pixels indicating smoldering. As Fig. 1 illustrates, the burned area approximates a circle. A radius was determined from a circular fit to the burned area, and the velocity was determined from the change in radius with respect to time. One experiment was performed for each data point. For a few conditions, multiple tests were performed, and these are reported as multiple data points. The results reported do not include the first 20 min to account for transient effects. The bias uncertainty of the mean propagation velocities is estimated at 2% based on the error in the calibration and linear fit. The errors in cellulose content and density are approximately 0.5% and 10 kg/m^3, respectively.

3. Numerical Model

A one-dimensional reactive porous media model was developed using the open-source software Gpyro [20, 21]. Gpyro solves one-dimensional transient equations which include condensed and gas-phase mass conservation and species conservation, as well as condensed-phase energy and gas-phase momentum equations. Thermal equilibrium is assumed between the gas and

solid phases. The reaction rates are expressed in Arrhenius form. The governing equations solved by Gpyro come from Lautenberger et al. [20]:

$$\frac{\partial \overline{\rho}}{\partial t} = -\dot{\omega}'''_{fg} \,, \tag{1}$$

$$\frac{\partial (\overline{\rho} Y_i)}{\partial t} = \dot{\omega}'''_{fi} - \dot{\omega}'''_{di} \,, \tag{2}$$

$$\frac{\partial (\overline{\rho}\overline{h})}{\partial t} = \frac{\partial}{\partial z}\left(\overline{k}\frac{\partial T}{\partial z}\right) - \dot{Q}'''_{s-g} + \sum_{k=1}^{K} \dot{Q}'''_{s,k} - \frac{\partial \dot{q}''_r}{\partial z} + \sum_{i=1}^{M} \left(\left(\dot{\omega}'''_{fi} - \dot{\omega}'''_{di}\right) h_i\right) \,, \tag{3}$$

$$\frac{\partial (\rho_g \overline{\psi})}{\partial t} + \frac{\partial \dot{m}''}{\partial z} = \dot{\omega}'''_{fg} \,, \tag{4}$$

$$\frac{\partial (\rho_g \overline{\psi} Y_j)}{\partial t} + \frac{\partial (\dot{m}'' Y_j)}{\partial z} = \dot{\omega}'''_{fj} - \dot{\omega}'''_{dj} - \frac{\partial}{\partial z}\left(\overline{\psi}\rho_g D \frac{\partial Y_j}{\partial z}\right) \,, \tag{5}$$

$$\dot{m}'' = -\frac{\overline{K}}{\nu}\frac{\partial P}{\partial z} \,, \text{ and} \tag{6}$$

$$P\overline{M} = \rho_g R T_g \,, \tag{7}$$

where ρ is the density, M is the number of condensed-phase species, $\dot{\omega}'''$ is the reaction rate, Y_j is the jth species mass fraction, h is the enthalpy, $\dot{Q}'''$ is the volumetric rate of heat release/absorption, $\dot{q}''_r$ is the radiative heat-flux, ψ is the porosity, K is the permeability/number of reactions, $\overline{M}$ is the mean molecular mass obtained from local volume fractions of all gaseous species, R is the universal gas constant, D is the diffusion coefficient, and P is the pressure. Subscripts f, d, i, j, k, s, and g are formation, destruction, condensed-phase species index, gas-phase species index, reaction index, solid, and gas (respectively). The overbar over h indicates averaged value weighted by condensed-phase mass fraction. The overbar over ρ, ψ, K, k indicates an averaged value weighted by condensed-phase volume fraction.

Temperature, reaction rates, mass fractions, and oxygen content were calculated by solving these governing equations. Downward propagation velocities were calculated using the location of the ignition temperature wave and compared with the experimental downward propagation. While the computational model shows all oxidation occurring at or near the highest temperature (rather than the ignition temperature), the ignition temperature was used to match the method used for experimental propagation. The average propagation velocity between 3 and 6 cm below the surface is reported.

The bulk densities of the cellulose and hemicellulose were assumed equal to the bulk density of the entire fuel. The densities of char and ash were calculated using the relation $\rho_{\text{char}} \approx 0.25 \times \rho_{\text{fuel}}$ [22] and $\rho_{\text{ash}} \approx \text{IC}/100 \times 10 \times \rho_{\text{fuel}}$ [23], where IC is the natural inorganic content. The ICs for cellulose and hemicellulose were set to 0.3% and 1.7% [24]. The values of the pore diameter, permeability, and parameter controlling the radiation heat transfer across pores of condensed-phase species were calculated using relations provided by Huang and Rein [8]. Other thermo-physical properties, which include solid density, thermal conductivity, and heat capacity of cellulose, hemicellulose, char, and ash, were obtained from literature [8, 25–29].

The reaction parameters of the global reactions used to represent smoldering in cellulose and hemicellulose come from the model for peat given by Huang and Rein [8]. For cellulose smoldering the value of stoichiometric coefficients (υ) were obtained from Kashiwagi and Nambu [30]. The stoichiometric coefficient of char from hemicellulose was obtained from Moriana et al. [24] while stoichiometric coefficients for ash were obtained by using the relation $\text{IC} = \upsilon_{\alpha,hp}\upsilon_{a,\alpha-co} = \upsilon_{a,ho}\upsilon_{a,\beta-co}$ for which the subscripts a, hp, ho, and co stand for ash, hemicellulose pyrolysis, hemicellulose oxidation and char oxidation, respectively. The values for $\upsilon_{\text{O}_2,k}$ were calculated using the relation $\upsilon_{\text{O}_2,k} = \Delta H/(-13.1)$ MJ/kg [9, 31, 32].

The global chemical reaction model used was also obtained from Huang and Rein [8]:

$$\text{C} \longrightarrow \nu_{\alpha,cp}\ \alpha\text{-Char}_c + \nu_{g,cp}\ \text{Gas} \tag{8}$$

$$\text{C} + \nu_{\text{O}_2,co}\ \text{O}_2 \longrightarrow \nu_{\beta,co}\ \beta\text{-Char}_c + \nu_{g,co}\ \text{Gas} \tag{9}$$

$$\alpha\text{-Char}_c + \nu_{\text{O}_2,c\alpha o}\ \text{O}_2 \longrightarrow \nu_{a,c\alpha o}\ \text{Ash}_c + \nu_{g,c\alpha o}\ \text{Gas} \tag{10}$$

$$\beta\text{-Char}_c + \nu_{\text{O}_2,c\beta o}\ \text{O}_2 \longrightarrow \nu_{a,c\beta o}\ \text{Ash}_c + \nu_{g,c\beta o}\ \text{Gas} \tag{11}$$

$$\text{HC} \longrightarrow \nu_{\alpha,hp}\ \alpha\text{-Char}_h + \nu_{g,hp}\text{Gas} \tag{12}$$

$$\text{HC} + \nu_{\text{O}_2,ho}\ \text{O}_2 \longrightarrow \nu_{\beta,ho}\ \beta\text{-Char}_h + \nu_{g,ho}\text{Gas} \tag{13}$$

$$\alpha\text{-Char}_h + \nu_{\text{O}_2,h\alpha o}\ \text{O}_2 \longrightarrow \nu_{a,h\alpha o}\ \text{Ash}_h + \nu_{g,h\alpha o}\ \text{Gas} \tag{14}$$

$$\beta\text{-Char}_h + \nu_{\text{O}_2,h\beta o}\ \text{O}_2 \longrightarrow \nu_{a,h\beta o}\ \text{Ash}_h + \nu_{g,h\beta o}\ \text{Gas} \tag{15}$$

where C and HC stand for cellulose and hemicellulose respectively, ν is the stoichiometric coefficient, α and β indicate char produced from fuel pyrolysis and oxidation reactions, respectively. Subscripts g, O_2, a, c, h, o, p, αo, βo are gas, oxygen, ash, cellulose, hemicellulose, oxidation, pyrolysis, α-char oxidation, and β-char oxidation, respectively.

The boundary and initial conditions are as follows: the ambient pressure and temperature were set to match the experiments: 1 atm and 293 K, respectively. The sample was ignited by setting a heat flux of 15 kW/m^2 at the top surface for 15 minutes, after which the flux stopped. At the top boundary the heat transfer coefficient and mass transfer coefficient was set to 10 $\text{W/m}^2\text{K}$ and 0.02 $\text{kg/m}^2\text{s}$, respectively [32]. The bottom surface was modeled to be insulated by setting a heat transfer

coefficient to 3 W/m^{2}K in order to take into account a small amount of heat transfer across the insulator. The mass flux across the bottom surface was set to zero [32].

4. Results and Discussion

4.1. Downward Smoldering

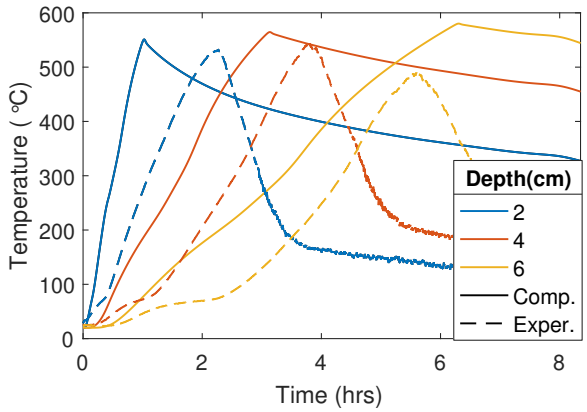

Figure 2: Temperature profiles calculated (solid lines) and measured (dashed lines) for three 2 cm depths for the duration of the burn, for 75% cellulose fuel with density at 300 kg/m^3.

Figure 2 compares calculated and measured temperatures at varying depths below the surface. Peak temperatures less than 600 °C are observed for both experiments and computations as a smoldering front propagates downward. In particular, the peak temperatures are similar at the depths closest to the surface. It is noted that peak temperatures increase with depth for the computational profiles, but decrease slightly for the experimental case due to heat losses. The slope of temperature profiles decreases with depth for both experimental and computational values.

Calculated and measured propagation downward velocities as the density and cellulose/hemicellulose content were varied are shown in Fig. 3. Downward smoldering tests were performed for 100%, 75%, and 50% cellulose fuels at densities ranging from 170–400 kg/m^3 for experiments and 275–400 kg/m^3 for computations. A larger total range of densities were evaluated experimentally because of physical imitations in the packing densities that could be achieved. As a result, a wider range of densities were necessary to obtain a similar change in density for the three fuel mixtures Two trends in the propagation velocities are apparent for both experimental and computational results. First, the velocities decrease with increasing density. Computationally, the propagation velocities reduce by roughly 40% over a 50% increase in fuel densities. The experimental propagation velocities decrease by about 50% for a 70% increase in density. Second, the velocities decrease with increasing cellulose content. Irrespective of density, the computational propagation velocities decrease by about 40% from 25% cellulose to 100% cellulose. Experimentally, the velocities change more: the propagation velocity decrease by roughly a factor of three from 50% to 100% cellulose. The larger sensitivity to fuel content and density in the experimental propagation velocities indicates that the model does not fully capture changes in the physical or chemical properties of the fuel, particularly for 100% cellulose. Nevertheless, the 50% and 75% cases fall within 20% of the computational velocities, indicating that the model generally captures the smoldering behavior. This is further supported by the similar trends in the experimental and computational propagation velocities.

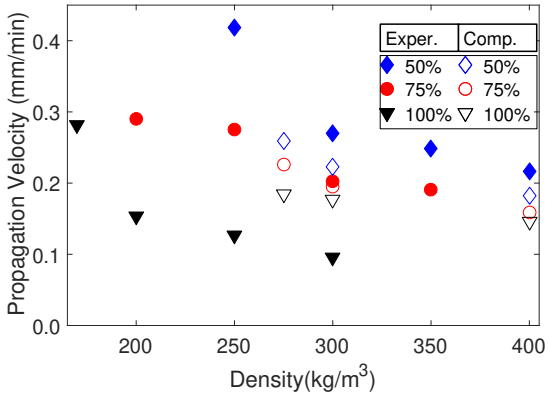

Figure 3: Computed and experimental vertical propagation velocities at varying cellulose content and densities.

To identify what causes the sensitivity of downward propagation velocity to fuel content, Fig. 4 shows the calculated pyrolysis and oxidation reaction rates and temperatures for varying fuel content with constant packing density. These reactions were evaluated because they are the dominant reactions in the smoldering simulation. The results are for 3.5 cm below the original surface; similar trends were observed at other depths. The density was held at 300 kg/m^3 for 50% and 100% cellulose (with remainder hemicellulose). The 50% cellulose case reaches its higher peak temperature more quickly, indicating a faster propagation velocity. Cellulose loses more mass during pyrolysis than hemicellulose, so more heat is released during oxidation[18] when more hemicellulose is present. The higher temperatures allow more heat to be conducted to the unburned fuel, increasing the propagation velocity. Hemicellulose also

pyrolyzes at a lower temperature and requires a lower activation energy for char [18, 19]. Thus larger concentrations of hemicellulose cause earlier mass loss and alpha-char production. This combined with the higher temperatures allows the fuel to oxidize more readily and propagate more quickly, as Fig. 4 shows.

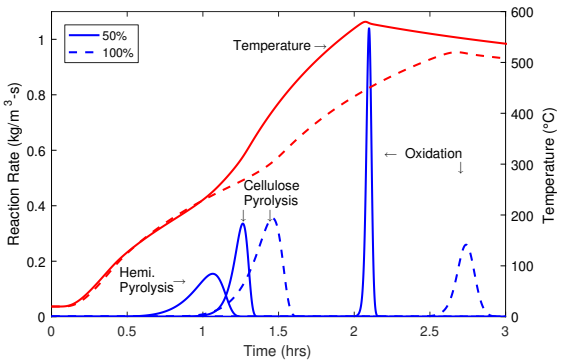

Figure 4: Reaction rates and temperatures of smoldering mixtures with a density of 300 kg/m^3 for 50% and 100% cellulose. The results were determined computationally.

To better understand the sensitivity of propagation rates to density, the reaction rates and temperatures were calculated for varying packing densities with constant fuel content, as shown in Fig. 5. Two different densities (300 and 275 kg/m^3) were evaluated for a mixture of 50% cellulose and 50% hemicellulose. The pyrolysis and oxidation at the lower density occur quicker than the higher density case. Note that the higher density has higher peak temperature as a result of lower heat losses relative to heat released. Despite the slightly higher peak temperature, which would increase propagation velocity, the propagation velocity actually decreases with density. This decrease in propagation velocity with density is attributed to changes in porosity and permeability, which limit oxygen diffusion. The less-dense fuel has a larger pore size, which allows oxygen to transport further into the char. This results in the fuel reacting earlier. The higher density also decreases the thermal diffusivity of the fuel, inhibiting heat transfer into the unburned fuel.

The decrease in smoldering propagation velocity with density is consistent with trends reported in literature. The sensitivity of smoldering propagation in cotton and pine needle beds to density is attributed to changes in permeability. At lower densities, air transports more readily through the porous fuel. As the fuel is compressed, the space between fuel particles becomes smaller, reducing oxygen availability below the surface [33, 34].

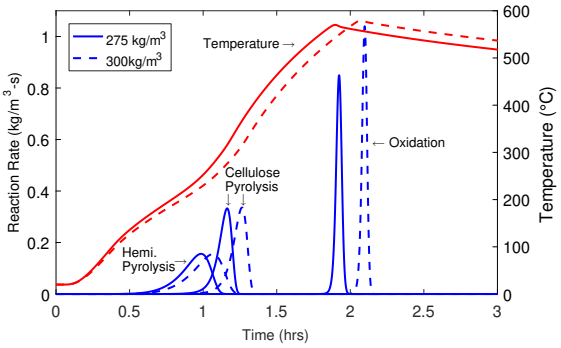

Figure 5: Computed reaction rates and temperatures for 50% cellulose and 50% hemicellulose at densities of 275 and 300 kg/m^3.

4.2. *Horizontal Smoldering*

Three-dimensional burns were conducted in an effort to identify the horizontal propagation characteristics of cellulose and hemicellulose, and to allow comparison with the downward smoldering propagation. The cellulose content was changed from 0 to 100% and the density was allowed to naturally vary during the first phase of testing. The resulting density varied from 175–725 kg/m^3. Figure 6 shows the horizontal propagation velocities for these tests. The velocity increases linearly with cellulose content, from about 0.3 mm/min with no cellulose to 1 mm/min for 75% cellulose (with remainder hemicellulose). However, the propagation velocity plateaus between 75 and 100% cellulose. This general trend of increased propagation velocity with cellulose content opposes that for downward propagation velocities. For comparison, the horizontal propagation velocity of peat (15–20% cellulose and 15–30% hemicellulose [35]) with a density equal to 116 kg/m^3 is near 0.7 mm/min [10], while the propagation velocity of cotton (90% cellulose) with a density equal to 100 kg/m^3 is between 1.3–1.5 mm/min [11].

To isolate chemistry effects the fuel content was varied and the density held constant. The fuels were tested at densities of 300 and 375 kg/m^3 with cellulose content ranging from 50 to 100%. Figure 7 shows the propagation velocity for these conditions. Note that it was not possible to test with a single density over the entire range of fuel contents because of physical limitations in packing. In general, propagation velocities decrease with increasing density and cellulose content, which is consistent with the trends in downward propagation velocity. Fuels with a density of 375 kg/m^3 typically propagated at velocities 10 to 20% lower than those with a density of 300 kg/m^3 with the same fuel content. The velocity decreases by roughly 35% over a 50% change in cellulose content (ρ = 300 kg/m^3). This trend, which

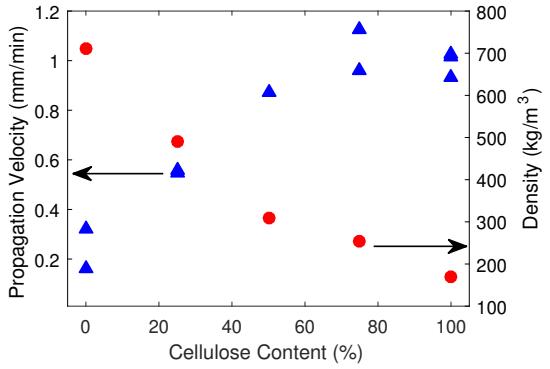

Figure 6: Experimental horizontal smoldering propagation velocities and densities for samples with cellulose content ranging from 0 to 100% (remainder hemicellulose). Triangles are propagation velocities and circles are densities.

is opposite of that observed when the density is allowed to vary naturally, is significant because it indicates that density is the dominant parameter causing the trends observed in Fig. 6. Specifically, as the cellulose content increases, the density of the mixture decreases and as as result the propagation velocity increases. The largest change in the propagation velocity occurs between 90% and 100% cellulose. This observation indicates a transition in the physical and chemical processes controlling smoldering propagation. This is not observed for the 375 kg/m^3 case because it could not be tested at cellulose contents greater than 75%.

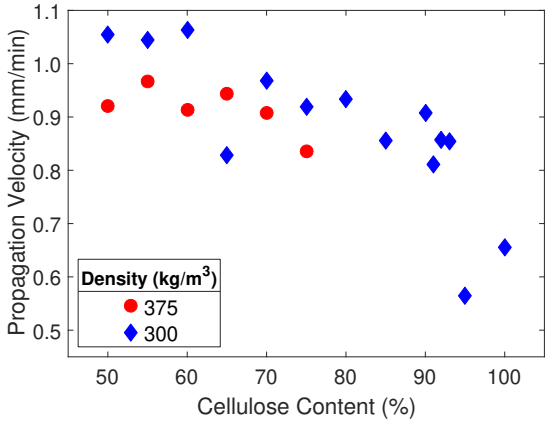

Figure 7: Experimental horizontal smoldering velocities at two densities for varying cellulose content (remainder hemicellulose).

To further isolate the effects of density on propagation velocity, experiments were conducted varying the density of samples with 100%, 75%, and 50% cellulose content (and the residual hemicellulose). Figure 8 shows the propagation velocities for these tests. For all three mixtures, the smoldering propagation velocity decreases with increasing density. However, the 100% cellulose case is much more sensitive to density changes than the other two fuel concentrations, as the propagation velocity decreases by approximately 40% over a 50% increase in density. In comparison, the propagation velocity decreases by roughly 20% for the 50% and 75% cellulose cases, indicating that the presence of hemicellulose reduces the impact of changs in density.

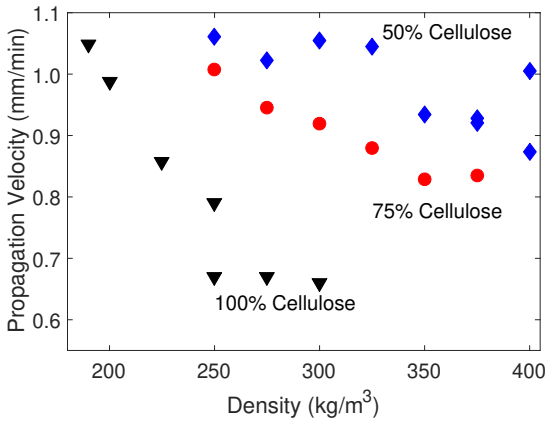

Figure 8: Horizontal propagation velocity determined experimentally for three mixtures of cellulose and hemicellulose at varying densities. Triangles = 100%, circles = 75%, and diamonds = 50% cellulose (remainder hemicellulose).

Figure 9 compares the experimental downward and horizontal smoldering propagation velocities. In general, the fuels smolder at least a factor of three faster horizontally than downward because of greater oxygen availability. Propagation velocities in either direction decrease with increasing cellulose content and density. Additionally, the 100% cellulose cases have the largest changes in propagation velocity with density in both directions. These similar trends with density and fuel content indicate common parameters controlling both horizontal and downward propagation.

5. Summary and Conclusions

The downward and horizontal smoldering propagation velocities were determined experimentally for binary mixtures of cellulose and hemicellulose with systematically varied densities. These fuels are of interest because they are major constituents within biomass. A one-dimensional computational model was used to determine corresponding downward propagation velocities and identify key physical processes.

Our specific conclusions from this work are as follows. 1) Smoldering propagation velocities of hemicel-

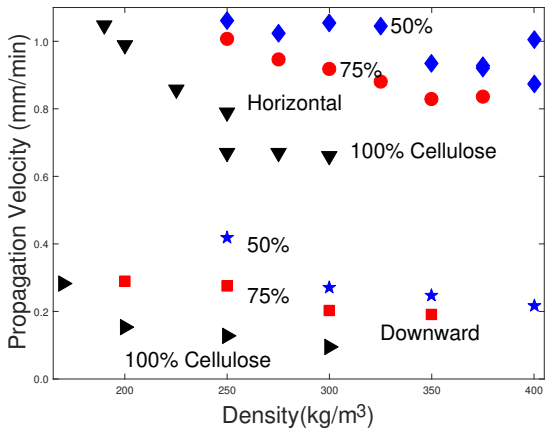

Figure 9: Measured horizontal and vertical propagation velocities determined experimentally for varying fuel content and densities.

lulose and cellulose decrease as the density of the fuel increases. Pure cellulose is more sensitive to changes in density than mixtures. The density sensitivity is attributed to changes in oxygen diffusion through the fuel. 2) Propagation velocities decrease with increasing cellulose content at a fixed density. This is attributed to the decreased heat release with increasing cellulose content, as well as cellulose's higher activation energy and slower pyrolysis compared with hemicellulose. 3) Propagation velocities increase as the cellulose content increases and the density of mixtures is allowed to vary without packing. This occurs because the effects of decreasing density dominate changes in propagation velocity as the cellulose content increases.

6. Acknowledgements

This research was funded by the Strategic Environmental Research and Development Program (SERDP) under contract number W912HQ-16-C-0045. The authors gratefully acknowledge the collaboration with Jim Reardon, Bret Butler, Wesley Page, and Wei Min Hao at the US Forest Service, as well as the generous assistance of Kaiden Moore and Jorge Dominguez-Baza in setting up and performing experiments.

The views, opinions, and/or findings contained in this report are those of the authors and should not be construed as an official Department of Defense position unless so designated by other official documentation.

References

[1] G. Rein, Smouldering Fires and Natural Fuels, Wiley, Oxford, pp. 15–33.

[2] T. Lee, A. P. Sullivan, L. Mack, J. L. Jimenez, S. M. Kreidenweis, T. B. Onasch, D. R. Worsnop, W. Malm, C. E. Wold, W. Min Hao, J. L. Collett Jr, J. L. Collett, Aerosol Sci. Tech. 449 (2010).

[3] R. Koppmann, K. Von Czapiewski, J. S. Reid, Atmos. Chem. Phys. Discuss. 5 (2005) 10455–10516.

[4] R. J. Yokelson, R. Susott, D. E. Ward, J. Reardon, D. W. T. Griffith, J. Geophys. Res. 102 (1997) 18865–18877.

[5] C. Liu, C. Zhang, Y. Mu, J. Liu, Y. Zhang, Environ. Pollut. 221 (2017) 385–391.

[6] L. M. Mckenzie, W. M. Hao, G. N. Richards, D. E. Ward, Environ. Sci. Technol. 29 (1995) 2047–2054.

[7] W. H. Frandsen, Can. J. Forest Res. 27 (1997) 1471–1477.

[8] X. Huang, G. Rein, Bioresour. Technol. 207 (2016) 409–421.

[9] X. Huang, G. Rein, Combust. Flame 161 (2014) 1633–1644.

[10] N. Prat-Guitart, G. Rein, R. M. Hadden, C. M. Belcher, J. M. Yearsley, Int. J. Wildland Fire 25 (2016) 456–465.

[11] B. C. Hagen, V. Frette, G. Kleppe, B. J. Arntzen, Fire Saf. J. 61 (2013) 144–159.

[12] B. C. Hagen, V. Frette, G. Kleppe, B. J. Arntzen, Fire Saf. J. 71 (2015) 69–78.

[13] J. Reardon, G. Curcio, R. Bartlette, Int. J. Wildland Fire 18 (2009) 326–335.

[14] W. H. Frandsen, Can. J. Forest Res. 17 (1987) 1540–1544.

[15] S. A. Waksman, Soil Sci. 41 (1936) 395.

[16] A. Gani, I. Naruse, Renew. Energy 32 (2007) 649–661.

[17] C. Quan, N. Gao, Q. Song, J. Anal. Appl. Pyrolysis 121 (2016) 84–92.

[18] H. Yang, R. Yan, H. Chen, D. H. Lee, C. Zheng, Fuel 86 (2007) 1781–1788.

[19] Z. Chen, M. Hu, X. Zhu, D. Guo, S. Liu, Z. Hu, B. Xiao, J. Wang, M. Laghari, Bioresour. Technol. 192 (2015) 441–450.

[20] C. Lautenberger, C. Fernandez-Pello, Fire Saf. J. 44 (2009) 819–839.

[21] C. Lautenberger, Gpyro v0.700, http://reaxengineering.com/trac/gpyro, 2009.

[22] X. Huang, G. Rein, Int. J. Wildland Fire 26 (2017) 907–918.

[23] X. Huang, Personal communication, 25 March 2017, 2017.

[24] R. Moriana, Y. Zhang, P. Mischnick, J. Li, M. Ek, Carbohydr. Polym. 106 (2014) 60–70.

[25] C-Therm Technology, Thermal Physical Properties Reference Library: Part II (L–R), http://ctherm.com/products/tci_thermal_conductivity/helpful_links_tools/thermal_physical_properties_conductivity_effusivity_heat_capacity_density2/, 2017. Accessed: 2017-08-29.

[26] R. Aseeva, B. Serkov, A. Sivenkov, Fire behavior and fire protection in timber buildings, Springer Series in Wood Science, Springer, Dordrecht, 2014.

[27] E. E. Thybring, J. Mater. Sci. 49 (2014) 1317–1327.

[28] J. Eitelberger, K. Hofstetter, Compos. Sci. Technol. 71 (2011) 134–144.

[29] R. T. Jacobsen, E. W. Lemmon, S. G. Penoncello, Z. Shan, N. T. Wright, in: A. Bejan, A. D. Kraus (Eds.), Heat Transfer Handbook, volume 1, John Wiley & Sons, 2003, pp. 43–160.

[30] T. Kashiwagi, H. Nambu, Combust. Flame 88 (1992) 345–368.

[31] C. Huggett, Fire Mater. 4 (1980) 61–65.

[32] X. Huang, G. Rein, Int. J. Wildland Fire 24 (2015) 798–808.

[33] B. C. Hagen, V. Frette, G. Kleppe, B. J. Arntzen, Fire Saf. J. 46 (2011) 73–80.

[34] M. El Houssami, J. C. Thomas, A. Lamorlette, D. Morvan, M. Chaos, R. Hadden, A. Simeoni, Combust. Flame 168 (2016) 113–126.

[35] D. M. S. Delicato, Physical-Chemical Properties and Sorption Characteristics of Peat, Ph. d., Dublin City University, 1996.